11-3

Effect of Atomic Interface on Tunnel Barrier in Ferroelectric HfO_2 Tunnel Junctions

Junbeom Seo and Mincheol Shin*
School of Electrical Engineering
Korea Advanced Institute of Science and Technology
Daejeon 34141, South Korea
*E-mail: mshin@kaist.ac.kr

***Abstract*— We have demonstrated the dependence of the atomic terminations on ferroelectric tunnel junctions (FTJs) based on ferroelectric HfO_2 using density functional theory calculation. The atomistic structures of HfO_2 FTJs with various interfaces are constructed and their device performances are calculated. We have found that the potential barrier is significantly tailored by atomic species of the terminating atom of HfO_2. In particular, the atomistic effect contributes to the electric field across the tunnel barrier, which leads to asymmetric behavior. We demonstrate that the ON/OFF current ratio of FTJs can be improved by adjusting the atomic terminations, albeit without the external asymmetric structure such as dissimilar metal electrodes and additional composite layers.**

Keywords—Ferroelectric tunnel junction, Schottky barrier, Ferroelectric HfO_2

I. Introduction

The recent discovery of the ferroelectric phase (space group: *Pca*2_1) of HfO_2 has provided a breakthrough for emerging memory and neuromorphic devices based on ferroelectric materials [1, 2]. Compared with perovskite oxide ferroelectric materials such as $BaTiO_3$ and $PbTiO_3$, excellent ferroelectric properties of HfO_2 can be retained with the thickness of few nanometers [2, 3]. Since HfO_2 is used in the commercial electronic devices, it is compatible with the Si-based CMOS process.

As one of the ferroelectric-based emerging memory devices, ferroelectric tunnel junctions (FTJs) have attracted much attention due to the high scalability and speed [4-7]. Since the concept of FTJs was proposed by L. Esaki in 1971 [4], the device based on $BaTiO_3$ has been demonstrated in the experiment [6]. A typical FTJ is composed of the ferroelectric thin film sandwiched between two metal electrodes as shown in Figure 1(a). The resistance states of FTJs can be achieved by varying the tunnel barrier with the polarization of the ferroelectric (See Figure 1(b)). This phenomenon is called the tunneling electro-resistance effect (TER).

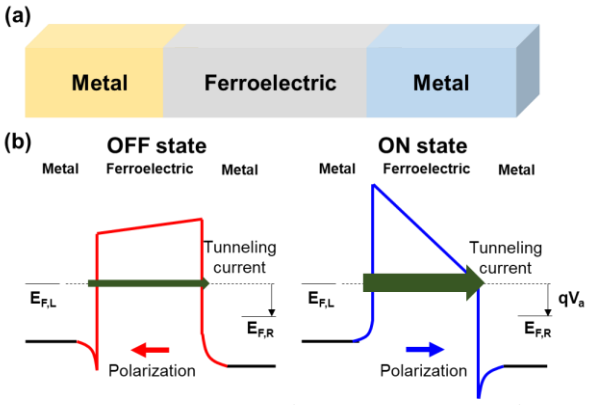

Figure 1. (a) Schematic structure of FTJ. (b) Band diagram of the FTJ under OFF and ON states.

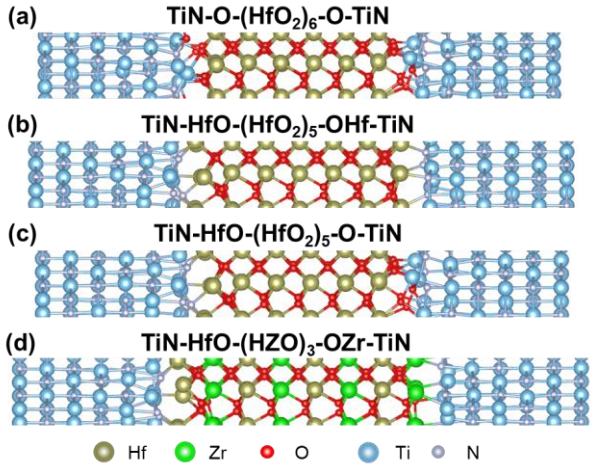

Figure 2. Atomistic structures of HfO_2-based FTJs. (a) O-terminated HfO_2, (b) Hf-terminated HfO_2, (c) Hf- and O-terminated HfO_2, and (d) Hf- and Zr-terminated HZO.

Recent studies have demonstrated FTJs with a HfO_2 film owing to excellent ferroelectricity in thin ferroelectric HfO_2 film [3, 7]. To utilize FTJs in practical applications, a high ON/OFF ratio of FTJs is required. For this purpose, asymmetric structures such as different metal electrodes, semiconductors, and additional composite layers have been considered [8, 9]. However, HfO_2-based FTJs still have shown a poor ON/OFF current ratio compared with perovskite oxide-based FTJs [7]. To further enhance the ON/OFF current ratio of HfO_2-based FTJs, the interface engineering between metal and ferroelectric layers can play a key role in modifying the barrier properties by adjusting the interface configuration [10]. However, to the best of our knowledge, there are few works which studied the effect of the interface on the tunnel barrier of HfO_2-based FTJs.

In this work, we investigate the effect of the terminated layers on the tunneling barrier of FTJs with a ferroelectric HfO_2 film using density functional theory (DFT) calculation. We focus on the influence of the atomic termination on the device performances. We construct the atomistic structures of FTJs based on HfO_2 and Zr-doped HfO_2 (HZO) with various atomic terminations. We reveal that the tunnel barrier is varied with the type of the atomic terminations of HfO_2, even leading to the asymmetric behavior of the tunnel barrier. Also, we report that without asymmetric metal electrodes and a composite layer, the ON/OFF current ratio of FTJs can be improved by adjusting the atomic termination at the interface.

II. Simulation Approach

All DFT calculations were performed by the SIESTA package [10]. We used the generalized gradient approximation (GGA) for exchange-correlation functional.

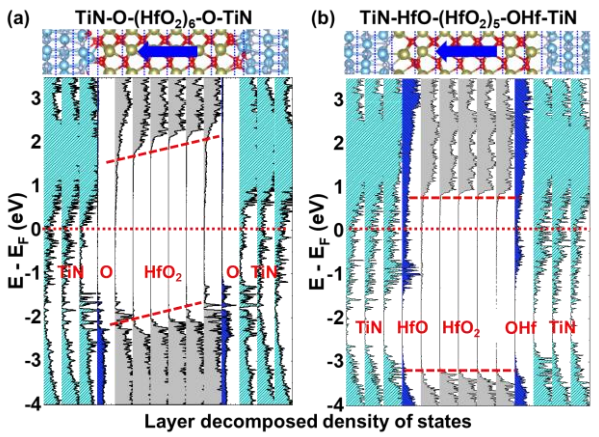

Figure 3. Layer-decomposed density of states of (a) OO and (b) HH structures. Blue thick arrows represent the polarization direction of HfO_2.

The Brillouin zone was sampled with the Monkhorst-Pack scheme with 5×5×1 *k*-points for the atomistic structures. Since the polarization of HfO_2 and HZO is oriented along the [001] direction, (001) surface of HfO_2 and HZO slab structures is in contact with the TiN electrodes. The atomistic structures are relaxed until the forces on each atom are less than 0.02 eV/Å. To explore the influence of the atomic termination of HfO_2 and HZO on the device performance, we constructed four types of the atomistic structures, namely, TiN-HfO-$(HfO_2)_5$-OHf-TiN, TiN-O-$(HfO_2)_6$-O-TiN, TiN-HfO-$(HfO_2)_5$-O-TiN, and TiN-HfO-(HZO)-OZr-TiN denoted by HH, OO, HO, and HZ, respectively, as shown in Figure 2. After the structural relaxation, we calculated the current-voltage characteristics using non-equilibrium Green's function implemented in the SIESTA package.

III. Results and Discussion

Depending on the atomic termination of the HfO_2, there are noticeable differences in the tunnel barrier. Figure 3 represents the layer-decomposed density of states (L-DOS) of the OO and HH structures under the same polarization state ($P_{\leftarrow}$). $P_{\leftarrow(\rightarrow)}$ represents the polarization pointing toward the left (right) direction. From this figure, the OO structure has a higher and steeper tunnel barrier compared with that of the HH structure. These discrepancies in the tunnel barriers between OO and HH structures are due to the dissimilar properties of interfacial charges.

A native polar surface of HfO_2 plays a key role in determining the interfacial charge properties, resulting in the modulation of the tunnel barrier. Figures 4(a) and (b) show the layer-resolved charges at the left and right interfaces between TiN and HfO_2 of the OO and HH structures. The atomic charges are calculated by Bader charge analysis [11]. As the electrons are transferred between interfacial atoms of TiN and HfO_2, non-zero charges are induced at the interfacial atoms. In the OO (HH) structure, the interfacial layers of HfO_2 are negatively (positively) charged, while the layers of TiN become positive (negative) (See Figures 4(a) and (b)). Note that such charge transfer generates the interface dipoles between the terminated atoms of HfO_2 and TiN [12], so that the electric field induced by the interface dipole affects the heights of the tunnel barrier. As shown in Figure 3, this explains that the O-terminated structure with negative charged interfacial layers shows a higher barrier height than that of the Hf-terminated structure with positively charged interfacial layers.

To explain the dependence of the electric field across the tunnel barrier on the terminating atoms of HfO_2, atomistic effects should be considered. The spontaneous polarization is induced by the movement of O atoms from the center of HfO_2, leading to the mismatch of the charges between the left and right terminated layers of HfO_2 and TiN. The polarization bound charges are incompletely screened by the metal electrodes inducing the depolarization field (E_{dep}). For simplicity, we assumed that E_{dep} depends on the metal properties, irrespectively of the terminated atoms of HfO_2. Also, the displacement of O atoms provides a discrepancy in the atomic charges between two terminated layers of HfO_2 (See Figures 4(a) and (b)). As we impose the additional intrinsic electric field (E_{int}) which is induced by this atomic

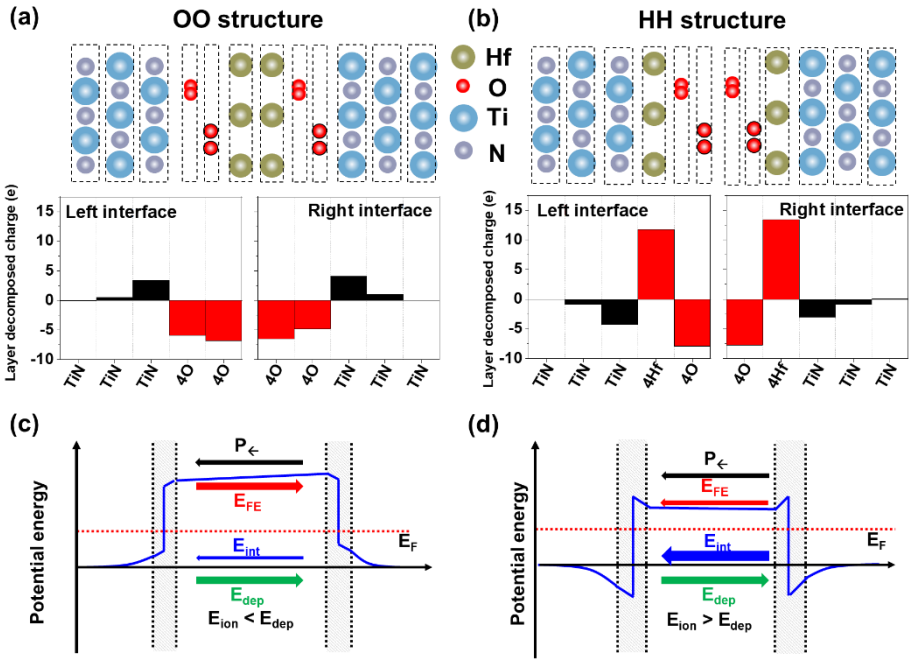

Figure 4. (a) and (b) Layer resolved atomic charges of the OO and HH structures, respectively. (c) and (d) schematic potential energy diagrams. The charge transfer occurs between the terminated layers of HfO_2 and TiN, which generate the interface dipoles. The polarization of the ferroelectric is imperfectly screened by TiN electrodes.

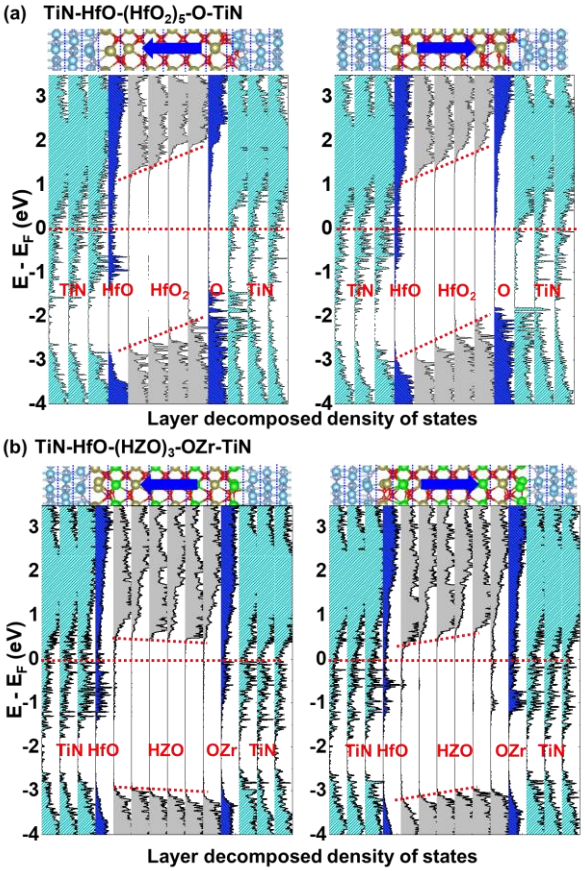

Figure 5. Layer-decomposed density of states of (a) HO and (b) HZ structures under $P_{\leftarrow}$ and $P_{\rightarrow}$ states.

charge difference, the total electric field (E_{FE}) across the tunnel barrier is given as

$$E_{FE} = E_{dep} + E_{int} + E_{bi} + E_a \quad (1)$$

where E_{bi} is the built-in field induced by the difference in the work function between metal and ferroelectrics and E_a is the external field. E_{bi} is zero because we considered the symmetric metal electrodes. If the atomistic effect is not considered, E_{int} is ignored and hence E_{FE} is dominated by E_{dep}. The large mismatch of the charges between two interfacial layers of HfO_2 leads to the large E_{int} of which the direction is opposite to E_{dep}. From Figures 4(a) and (b), it can be seen that the charge mismatch of the HH structure is larger than that of the OO structure. It means that the HH structure has a stronger E_{int} than that of the OO structure. E_{FE} of the HH structure becomes weak and opposite to the direction of E_{dep} because E_{int} is large enough to overcompensate E_{dep}, but in the OO structure, E_{FE} is the same direction to E_{dep} due to weak E_{int}.

Based on the atomic charge properties of the terminated layer of HfO_2, an asymmetry between the left and right barrier heights can be achieved, which is analogous to the effects of the disparate metal electrodes. Figure 5 shows the L-DOS of the HO and HZ structures. As shown in Figure 5(a), the HO forms asymmetric terminated layers of which the tunnel barrier is not modulated by varying the polarization. However, as seen in Figure 5(b), although the interfacial layers of the HZ structure are asymmetric, the electric field across the ferroelectric layer is switched by the polarization reversal.

Figure 6 represents the layer resolved atomic charges of the HO and HZ structures. As shown in Figure 6(a), the HO

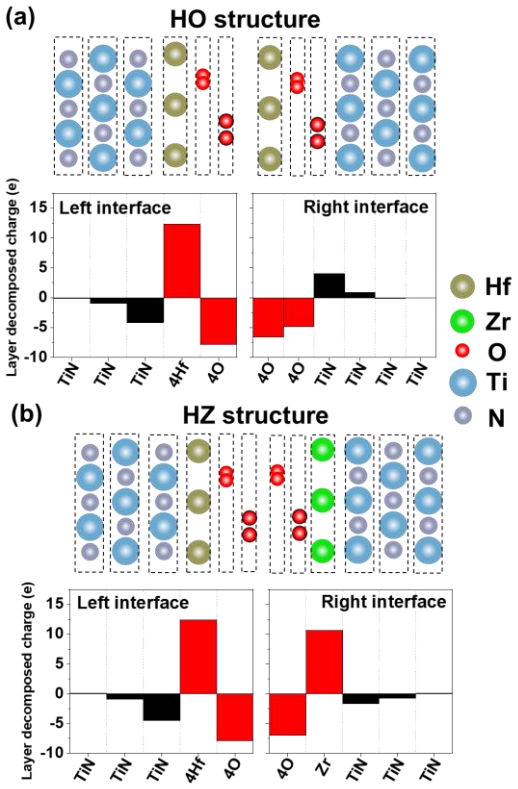

Figure 6. Layer-resolved atomic charges at the interfaces of (a) OO and (b) HZ structures, respectively.

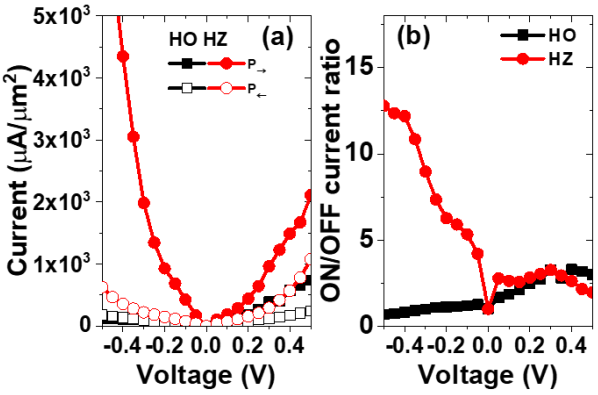

Figure 7. (a) Current-voltage characteristics and (b) ON/OFF current ratio of HO and HZ structures.

structure has a large difference in the interfacial charges between Hf and O layers, leading to large E_{int} which is not switched by the polarization reversal. Non-switchable E_{int} of the HO structure makes the tunnel barrier independent of the polarization states. However, as shown in Figure 6(b), in the case of the HZ structure, atomic charges of both terminated layers are positive, but their difference is small enough so that E_{int} can be switched by the polarization reversal.

Figure 7 represents the current-voltage characteristics and ON/OFF current ratio of the HO and HZ structures. Although HO and HZ structures form the asymmetric tunnel barrier, the HO structure leads to a low ON/OFF current ratio of about 3, but the ON/OFF current ratio of the HZ structure reaches to 12. This is because the tunnel barrier of the HO structure is not altered by the polarization reversal. In contrast, the left and right barrier heights of the HZ structure are asymmetrically

varied with the polarization. This means that the difference in tunneling current between ON and OFF state can be achieved, resulting in the large ON/OFF current ratio. This result shows that without the symmetric metal electrodes or additional composite layers, the ON/OFF current ratio can be improved.

IV. Conclusion

We investigated the effect of the interface configuration of HfO_2 on the tunnel barrier using DFT simulation. We have found that the interface charge properties are highly dependent on the terminated layer of HfO_2. Therefore, by adjusting the type of the terminated layer, one can produce the large ON/OFF ratio, albeit without either asymmetric metal electrodes or an additional composite barrier. Our findings may provide the guideline for the device fabrication to achieve a high ON/OFF ratio in FTJ devices.

Acknowledgment

This work was supported by Samsung Research Funding and Incubation Center of Samsung Electronics under Project Number SRFC-TA1703-10.

References

[1] T. S. Böscke, J. Müller, D. Bräuhaus, U. Schröder, and U. Böttger, "Ferroelectricity in hafnium oxide thin films," Appl. Phys. Lett. vol. 99, 102903, 2011.

[2] S. J. Kim, J. Mohan, S. R. Summerfelt, and J. Kim, Jom, "Ferroelectric $Hf_{0.5}Zr_{0.5}O_2$ thin films-A review of recent advances," vol. 71, pp. 246-255, 2019.

[3] S. S. Cheema, *et al.*, "Enhanced ferroelectricity in ultrathin films grown directly on silicon," Nature, vol. 580, no. 7804, pp. 478–482, 2020

[4] L. Esaki, R. B. Laibowitz, and P. J. Stiles, "Polar switch," IBM Tech. Discl. Bull, 1971

[5] E. Y. Tsymbal and H. Kohlstedt, "Tunneling across a ferroelectric," Science, vol. 313, no. 181, 2006.

[6] A. Gruverman, D. Wu, H. Lu, Y. Wang, H. W. jang, C. M. Folkman, M. Ye. Zhuravelv, D. Felker, M. Rzchowski, C. B. Eom, and E. Y. Tsymbal, "Tunneling Electroresistance Effect in Ferroelectric Tunnel Junctions at the Nanoscale," Nanoletters, vol. 9, no. 9, pp. 3539-3543, 2009.

[7] Z. Wen and D. Wu, "Ferroelectric tunnel junctions: Modulations on the Potential Barrier," Adv. Mater., 1904123, 2019

[8] J. Yoon, S. Hong, Y. W. Song, J. Ahn, and S. Ahn, "Understanding tunneling electroresistance effect through potential profile in $Pt/Hf_{0.5}Zr_{0.5}O_2/TiN$ ferroelectric tunnel junction memory," Appl. Phys. Lett., 115, 153502, 2019

[9] B. Max, M. Hoffmann, S. Slesazeck, and T. Mikolajick, "Ferroelectric tunnel junctions based on ferroelectric-dielectric $Hf_{0.5}Zr_{0.5}.O_2/A1_2O_3$capacitor stacks," European Solid-State Device Research Conference, pp. 142–145, Sep. 2018

[10] J. M. Soler, E. Artacho, J. D. Gale, A. García, J. Junquera, P. Ordejón, and D. Sánchez-Portal, D, "The SIESTA method for ab initio order-N materials simulation," Journal of Physics: Condensed Matter, vol. 14, no. 11, 2745, 2002.

[11] G. Henkelman, A. Arnaldsson, and H. Jónsson, "A fast and robust algorithm for Bader decomposition of charge density," Computational Materials Science, 36(3)," pp. 354-360, 2006.

[12] R. T. Tung, "Recent advances in Schottky barrier concepts," Materials Science and Engineering: R: Reports, vol. 35, pp. 1-138, 2001